Fusion Reactors: Their Challenge to Materials Scientists

G.L. Kulcinski

October 1978

UWFDM-277

Contemp. Phys. 20, 417 (1979).

FUSION TECHNOLOGY INSTITUTE

UNIVERSITY OF WISCONSIN

MADISON WISCONSIN

Fusion Reactors: Their Challenge to Materials Scientists

G.L. Kulcinski

Fusion Technology Institute
University of Wisconsin
1500 Engineering Drive
Madison, WI 53706

http://fti.neep.wisc.edu

October 1978

UWFDM-277

Contemp. Phys. 20, 417 (1979).

CONTEMP. PHYS., 1979, VOL. 20, NO. 4, 417–447

Fusion Reactors: their Challenge to Materials Scientists

G. L. KULCINSKI

Department of Nuclear Engineering, University of Wisconsin, Madison, Wisconsin 53706, USA

ABSTRACT. The environment of a DT fusion reactor is unlike anything previously experienced in fission reactors and the requirements for first wall materials will be quite severe. Considerable emphasis is placed on characterizing the environment for both magnetically and inertially confined plasmas, focusing on what we do and do not know at the present time. Once the neutron, photon, and charged particle fluxes are determined, the primary damage functions are calculated and it is shown that the displacement rate in inertial confinement fusion reactors and the helium production rate in all DT fusion reactors are sufficiently different to warrant concern over extrapolation from present facilities. Finally, the major responses of the first wall to the primary damage state appear in the swelling and embrittlement problems. Observations on potential materials and their operating limits are also made.

1. Introduction

Several recent successes in the fusion research programmes around the world have strengthened the earlier predictions of scientists that the scientific feasibility of this important new energy source will be demonstrated early in the 1980's. The achievement of ion temperatures near ignition in the magnetically confined plasmas of Tokamak (Eubank *et al.* 1978) and Mirror (Simonen *et al.* 1978) test facilities as well as the encouraging experimental results in the inertially confined pellet-fusion programme using lasers (Emmett 1978) and electron beams (Aranchuk *et al.* 1978) has stimulated the thinking of governments and electric utility leaders alike toward the ultimate use of this energy source.

Anticipating this breakthrough in plasma research, many technology oriented groups began in the early 1970's (Badger *et al.* 1973, Mills *et al.* 1974, Werner *et al.* 1974, Ribe 1974, Fraas 1973, and Booth 1972), to conduct commercial reactor design studies based on the eventual successful confinement of a deuterium-tritium (DT) plasma. These reactor designs were used as 'problem finders' to identify the most critical problems that need to be solved as the fusion programme transcends the physics phase and enters the engineering phase. At the top of almost every list of non-plasma-physics-related problems was the question of the successful performance of the fusion reactor materials over the lifetime of the reactor. In fact such problems have been labelled as "the second most serious obstacle to the commercialization of fusion power".

There are two major reasons why the materials problem in general, and the problem of the first wall in particular (defined as that solid structure which directly faces the plasma), rate such a high level of concern. The first is that, in contrast to fission reactors, the radiation environment is not very well established. This is especially true for the laser fusion approach because much of the data on output spectra is classified by the governments sponsoring the research. Needless to say, it is extremely difficult to be specific about the exact materials design when one doesn't even know the details of the radiation environment in which the materials are to

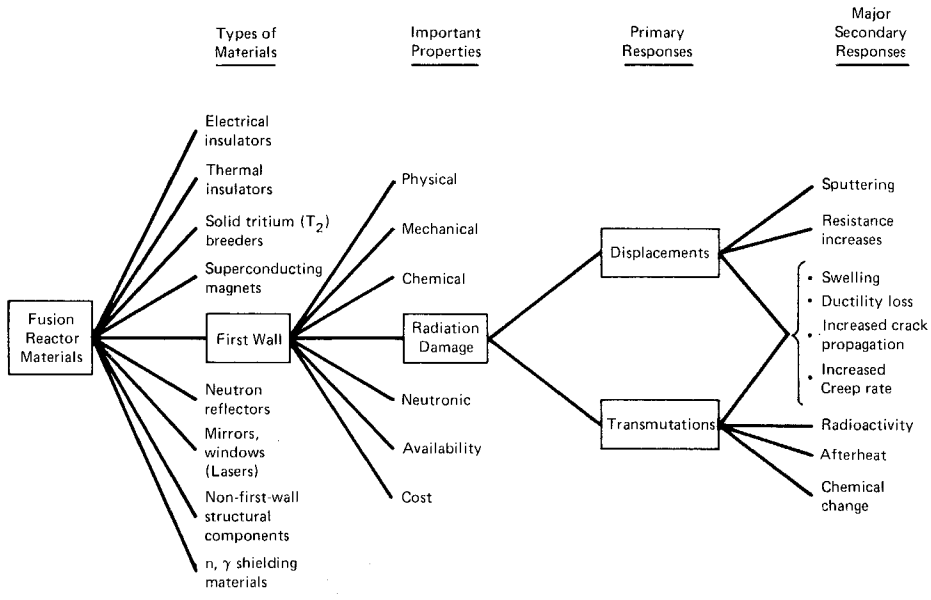

Fig. 1. Scope of fusion materials problems considered in this article.

perform. The second reason for the concern over the materials problems is that there are presently *no* test facilities that can simulate the entire radiation environment to a first wall structure. This is equally true for both the magnetic and inertial confinement approaches. In fact, the highest known exposure of any material with 14 MeV neutrons would be comparable to only a few hours of operation in a large power reactor.

On top of these uncertainties one finds a wider range of materials requirements than is the case in fission reactors. As a prelude to the body of this paper, the reader is asked to study the scope of the materials problems as outlined in fig. 1. There are approximately 10 classes of materials which are expected to perform in the irradiation environment of a fusion reactor compared to approximately five (fuel, cladding, core structure, control rods, pressure vessel) in fission facilities. The reader is referred to previous reviews that outline the general design criteria for the various fusion reactor materials (Kulcinski 1975, 1978a, 1978b, 1979, Wiffen and Stiegler 1977, Hovingh 1977).

The object of this article is to concentrate on perhaps the most critical materials problem; that of the first walls which face the plasma directly. These walls will experience the highest neutron, charged particle and X-ray fluxes in the reactor and therefore represent perhaps the weakest link in the design. These walls must endure such extreme conditions while maintaining good vacuums (ranging from $\sim 10^{-5}$ Torr in magnetically confined systems to $\gtrsim 1$ Torr in some inertial confinement fusion systems) and not interfer with, or contaminate the plasma. They must contain sometimes corrosive, or high pressure coolants under rapidly varying stresses for as many as hundreds to several millions of pulses per year.

The choice of the appropriate first wall material depends on at least seven major factors as outlined in fig. 1. A more complete discussion of these factors is given elsewhere (Badger *et al.* 1976) but it is important for our purposes here to remember that one cannot make a decision based on only one or two of these factors; the

ultimate material will be the best compromise on all seven. Without repeating the results of previous work, we list below the current view of the most appropriate material–temperature combinations.

First wall operating range of temperature	Material
Room temperature to 200°C	*Aluminum alloys*
300–500°C	*Austenitic steels*
	Titanium alloys
500–800°C	*Vanadium alloys*
800–1000°C	*Molybdenum and molybdenum alloys*
1000–1500°C	*Graphite*

Finally, since radiation damage seems to be the most limiting barrier to the successful operation of a first wall we will concentrate our attention in that area for the rest of this report. The remainder of this paper is organized as follows: First, the unique radiation damage environment is examined in some detail because it is the basis for the defect production calculations that will follow. We will then examine the response of metals to the defects as a prelude to some general remarks on first wall lifetime estimates. The reader will note that at times we must treat magnetic confinement fusion reactors apart from inertial confinement fusion reactors because of their vastly different operating characteristics. More background on the design features of these two classes of reactors can be found in IAEA sponsored workshops in Culham (1974) and Madison (1978).

2. Radiation damage environment from a DT plasma

The fundamental reaction to consider in early fusion plasmas is:

$$^{2}_{1}\mathrm{D} + ^{3}_{1}\mathrm{T} \rightarrow ^{4}_{2}\mathrm{He}(3{\cdot}52\,\mathrm{MeV}) + ^{1}_{0}\mathrm{n}(14{\cdot}08\,\mathrm{MeV}) \qquad (1)$$

This reaction is either produced in a magnetically confined plasma or in the core of a pellet compressed to very high densities by laser light or charged particles.

There are basically two types of magnetically confined plasma devices that are being studied today; Mirrors and Tokamaks. Both of them rely on magnetic fields to constrain the trajectory of the high temperature ($\sim 100\,000\,000$ K) D^+, T^+, and He^{2+} ions so that they do not touch the first wall and cause it to melt. The Mirror concept uses a cylindrical magnetic bottle configuration in which the field is higher at the open ends to reduce the leakage of plasma particles. The Tokamak concept employs a toroidal geometry in which the magnetic field lines close on themselves so that there is no leakage of the particles out of the 'end'. The only way particles leak out of the Tokamak plasma is if they are scattered out of the reaction zone by collision with other plasma ions.

The second major approach to fusion is to compress deuterium and tritium to very high densities ($\sim 1000\,\mathrm{g\,cm^{-3}}$) and temperatures with high intensities of charge particles or laser light. Such a mechanism holds the fuel together long enough for more energy to be released than was invested in the compression and thus it is sometimes called the inertial confinement approach. Typically the reaction chamber is spherical in geometry with the lasers or accelerators located outside. The laser light is directed to a pellet of D and T (along with other coatings, see Section 2.2) via mirrors, while charged particles may be directed from diodes or guided by magnets.

In all three of these devices there are three major forms of radiation emitted from the plasma that could reach the reaction chamber first wall. They are:

Photons (X-rays ranging from a few eV in magnetically confined plasmas up to 100–10 000 eV or more from pellets).

Energetic neutral or charged particles (unburnt fuel such as D and T, helium ions, and non-fuel pellet debris ranging from H, Be, C, O, Si, Fe to as high as U).

Neutrons.

To some degree, the amounts of energy in charged particles or photons are not independent as the X-rays originate from the acceleration or deceleration of the ions. The total energy in photons depends on many things, such as the magnetic field and degree of collisionality so that there are no 'unique' photon or particle spectra. Therefore, we will be forced to choose some representative spectra from the recent literature and the reader should recognize that these spectra could be different from those eventually found in a working reactor. To make things clearer let us treat the neutrons separately from the charged particles.

2.1. *Neutron environment*

2.1.1. *Neutron spectra*

Neutrons from a DT reaction do not have a monoenergetic energy as indicated in eqn. (1), but rather a distribution of energies around 14·08 MeV due to the relative velocity of the reacting fuel ions and the angle of recoil of the helium atoms. A typical neutron spectrum from a reacting plasma is shown in fig. 2.

When the neutrons are born inside a highly compressed pellet, they could suffer many collisions with the pellet material before they reach the first wall. An example of a downscattered spectrum associated with such collisions is also shown in fig. 2 where ρ is the density in g cm^{-3} and R is the radius in cm of the fuel pellet during the

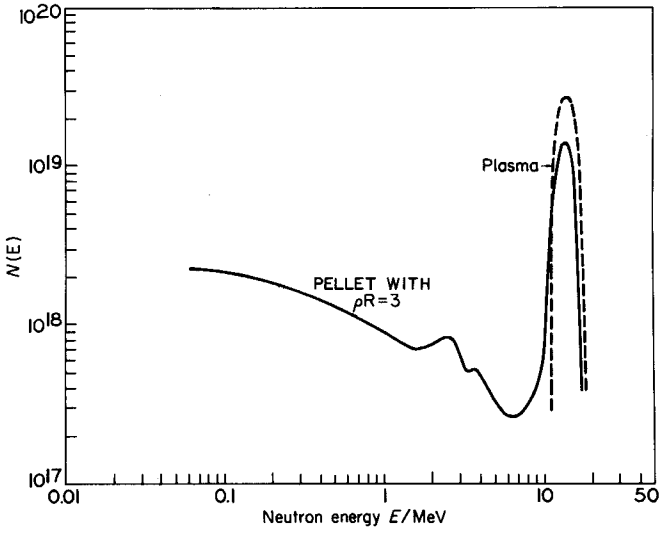

Fig. 2. Typical neutron spectra from DT reacting plasmas $\rho r = 3$ means that the product of the density (in g cm^{-3}) and the radius (in cm) of the pellet at that density equals 3 g cm^{-2}.

burn (Beranek 1978). Not only is the average DT neutron energy lowered, but the energy distribution is broadened down to as low as a few hundreds of keV.

Fig. 2 represents only the energy spectra of the neutrons incident on the first wall (i.e., the current) and the flux of neutrons to the first wall must include those neutrons backscattered from the blanket or downscattered in the first wall. An example of the total neutron energy spectrum for a lithium-cooled, 316 stainless steel blanket structure bombarded with 14·1 MeV neutrons from a diffuse plasma source is shown in fig. 3. We quote numbers here for 1 MW of 14·1 MeV neutrons passing through one square metre, which is equal to $4{\cdot}43 \times 10^{13}$ n cm^{-2} s^{-1}. Note that neutron energies now extend all the way down to less than 1 keV with a substantial number of neutrons in the 0·1 to 1 MeV range. In fact, we find that the total flux of neutrons is 5–8 times the current of 14·1 MeV neutrons. This fusion spectrum is also compared to that in a fast (EBR-II)† and thermal (HFIR)‡ fission reactor in fig. 3. The main differences are in the high energy tail (> 10 MeV) for fusion and the large number of neutrons at low energies in thermal fission reactors. One also should note that at a wall loading of 1 MW m^{-2}, which is perhaps the lower limit for economical fusion power plants, the total neutron flux is much *lower* in fusion reactors than in fission reactors.

2.1.2. *Neutron fluxes*

Typical fusion reactor designs have considered neutron wall loadings of 1 to 10 MW m^{-2}, with the upper limit usually set by thermal stress considerations (see

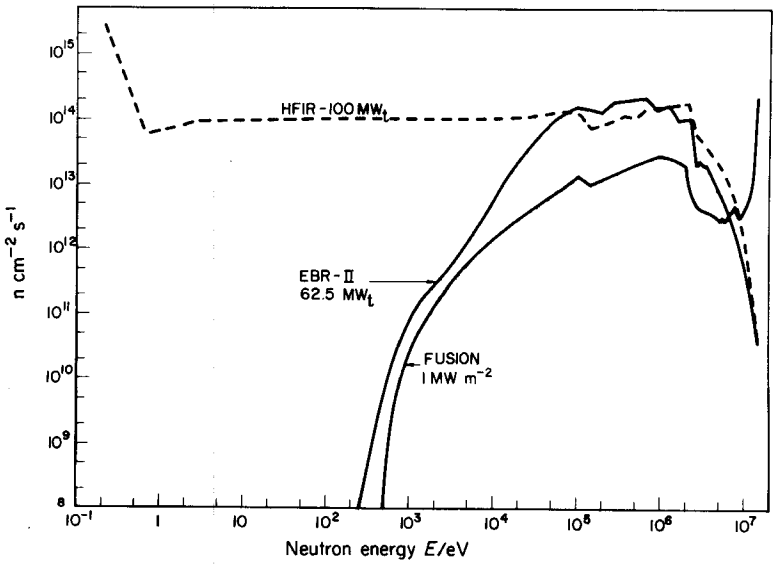

Fig. 3. A comparison of the neutron spectra in various nuclear facilities.

† EBR-II—Experimental fast breeder reactor, Idaho Falls, U.S.A., 62·5 MW.

‡ HFIR—High neutron flux materials research reactor, Oak Ridge National Laboratory, U.S.A., 100 MW$_t$, 5×10^{15} n cm^{-2}s (thermal).

Section 2·3). If all of the energy in the charged particles is incident on the first wall (either by conversion to bremsstrahlung or through charged exchange reactions to produce energetic neutral atoms) this upper limit ranges from as low as 2 to 3 MW m^{-2} for 316 SS to as high as 10 MW m^{-2} for V-20Ti (Conn 1978). Hence we can limit our discussions to 1–10 MW m^{-2}. At these wall loadings in a magnetically confined DT plasma reactor, the 14·1 MeV neutron current ranges from 4×10^{13} to 4×10^{14} n cm^{-2} s^{-1} while the total neutron flux of all energies could range from 2×10^{14} to 2×10^{15} n cm^{-2} s^{-1}.

In the simple or tandem mirror reactor designs, the neutron flux is anticipated to be constant with time while for Tokamaks, the neutron flux is anticipated to be constant only for periods of 1 to 100 minutes depending on the method of impurity control or the magnitude of the power swing in the transformer magnets (table 1). The downtime between each pulse should be small enough such that the duty cycle is >90%. This means that there will be periods of 5 to 500 seconds when no neutrons strike the first wall of a Tokamak and annealing of the damage can take place.

Table 1. Typical fluxes of neutrons to the first walls of fusion reactors.

	Approximate neutron flux (n cm^{-2} s^{-1} per MW m^{-2})		Chronology	
Reactor type	14·1 MeV	Total	Steady state period	Time between pulses
Tokamak	4×10^{13}	2×10^{14}	1–100 minutes	5–500 seconds
Mirror	4×10^{13}	2×10^{14}	Weeks to months	—
Laser	10^{20}–10^{21}†		10^{-8} to 10^{-7} second	0·1 to 1 second
		$\sim 5 \times 10^{19}$ to 5×10^{20}†	$\sim 10^{-6}$ second‡	0·1 to 1 second
	$< 4 \times 10^{13}$§‖	2×10^{14}§	Not applicable	Not applicable

† Instantaneous rate following microexplosion.
‡ Includes downscattered and backscattered neutrons.
§ Averaged over 1 second of operation.
‖ Depends on the degree of downscattering.

A completely different situation exists in the inertial confinement systems. Because the energy is released in a microexplosion during $\sim 10^{-11}$ seconds, the neutrons arrive in tremendous bursts. If the neutrons were absolutely monoenergetic, they would arrive over a $\sim 10^{-11}$ second time period. However, due to the Doppler broadening alone, the time spread of the neutron arrival at the first wall of a typical size chamber (~ 5 m radius) is ~ 50 ns. This means the current of 14·1 MeV neutrons will be between 10^{20} and 10^{21} n cm^{-2} s^{-1} for a short period of time depending on the pellet design. The time between the bursts depends on many parameters such as power level, time required to prepare the chamber for another 'shot', etc., but it ranges from approximately 0·1 to 1 second. The reader will recognize from the above discussion and table 1 that the time history of neutron damage in this type of reactor is completely different from anything encountered up to this time in fission reactors.

2.1.3. *Spatial effects*

If the reaction chamber were cylindrical around a line source (as may be the case for Mirror reactors) or spherical around a point source (e.g., laser fusion) the neutron

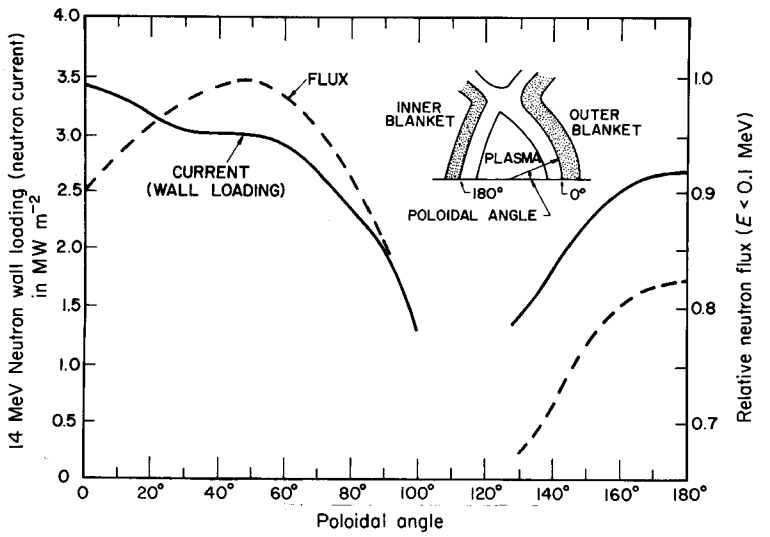

Fig. 4. Poloidal variations of neutron wall loading and flux in UWMAK-III.

flux would be uniform around the first wall. However, cylindrical chambers have been proposed for inertial confinement systems so the neutron flux to the first wall will vary by as much as a factor of 2 to 4 from a maximum at the midplane to a minimum at the ends of the chamber. A much more complicated geometry is associated with the toroidal geometry of the Tokamak. In this system, the neutron flux and currents are *not* the same and there can be rather complex variations around the poloidal directions. Furthermore, for physics reasons, it has become advantageous to elongate the plasmas such that the vacuum chambers are no longer circular in cross section, but can have shapes such as that shown in fig. 4 for a recent Tokamak reactor design UWMAK-III (Badger *et al.* 1976). The neutron wall loading (a measure of the neutron current) peaks at the midplane and drops off as one moves in the poloidal direction. On the other hand, the neutron flux peaks at $\theta \sim 60°$, almost 40% higher than at the midplane. It is the latter quantity that is important for damage calculations.

The point of the above comparison is to illustrate that there will be a highly non-uniform damage rate around the plasma chamber which could induce severe stress gradients. Furthermore, such non-uniform damage could require early replacement of some first wall components which have not yet reached their normal end-of-life capabilities. More about this later.

2.2. *Charged particle and neutral atom spectra*

Roughly 20% of the thermonuclear energy from the DT reaction will end up in charged particles, neutral atoms or X-rays. In a magnetically confined plasma, the energy flux to the wall is more likely to be made up of charge-exchange neutral atoms because of the good magnetic confinement of charged particles. Ideally one would like the kinetic energy of the 3·5 MeV helium atoms to be converted to X-rays which could be absorbed uniformly by the first wall rather than to let the energetic helium ions strike the wall. However a low density of neutral atoms (e.g., D^0, T^0, etc.) will surround and to some degree permeate the plasma and these neutral atoms can

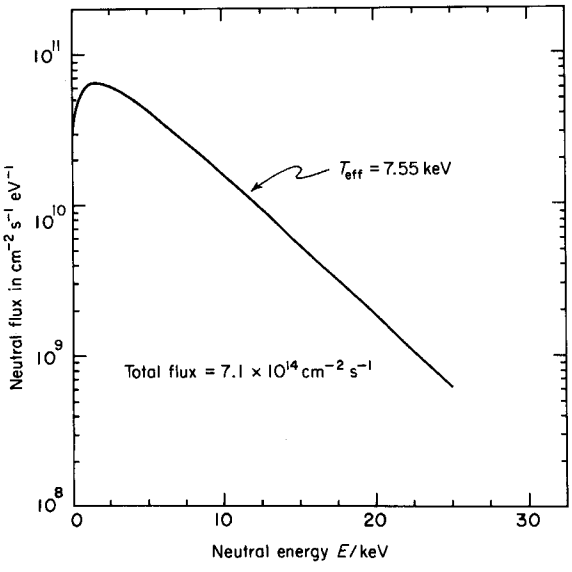

Fig. 5. D-T neutral flux to liner in UWMAK-II.

acquire sufficient kinetic energy through collisions with charged particles in the plasma to impact the first wall. An example of the flux of such neutrals to be expected from a DT plasma is shown in fig. 5 (Conn and Kesner 1976). This figure demonstrates that while the average neutral energy may be in the 5–10 keV range some particles strike the wall with tens of keV energy. A more recent reactor design (Conn, Kulcinski and Maynard 1978) utilized a cold gas around a Tokamak plasma to lower the average energy of the neutral atoms. However, such a lowering of the average energy is also accompanied by an increase in the flux of neutrals so that the heat load may still be substantial, especially to the safety devices preventing the plasma from striking the first wall.

The ion flux to the first wall of a mirror reactor is expected to be much lower than for a Tokamak but it will consist of higher energy particles. As we move to other parts of the mirror reactor one finds that the problems are quite different in the end plugs and direct converters and the reader is referred to Moir (1976) for more details about those conditions.

The particle flux to the first walls of inertial confinement reactors is likely to be made up of charged particles with much wider mass and energy variations. The mass variation stems from the requirements of pellets (as currently designed) to have low-mass ablative coatings, high-Z tampers, and DT mixtures such as shown in fig. 6 (Nuckolls. to be published). Since there are generally no externally applied magnetic fields, all of the ions from the pellet will be directed out toward the first wall and, in the absence of liquid metal coatings on the wall or high gas chamber pressures, they will impinge directly on the wall. Table 2 gives a possible spectrum for a much simpler pellet (Hunter and Kulcinski 1978a). A partially thermalized helium component is included to model fast alphas and silicon is used to model the atoms of medium mass number. The variation in energy stems from the fact that the various components of the particle debris (except for the helium) generally have the same blow-off velocity, and hence higher energies for higher mass particles.

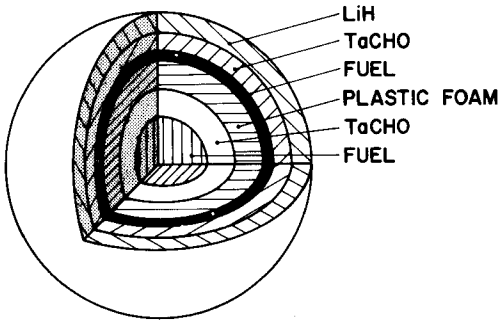

Fig. 2. Schematic of high gain DT fusion pellet. TaCHO is the code name for a tantalum carbonyl, this is *not* its exact chemical formula.

Table 2. Possible particle spectra from a 100 MJ pellet.

Component	Energy (MJ)	Energy spectrum
Laser	0·2	10·6 μm
X-ray	2·0	1 keV-BB
Deuterium	4·6	160 keV-M
Tritium	6·9	240 keV-M
Helium (thermalized)	1·2	320 keV-M
Helium (fast)	5·4	$2 \pm 0{\cdot}5$ MeV-G
Silicon	2·7	800 keV-M
Neutrons	77	14 ± 1 MeV-G
	100·0	

BB = blackbody, M = Maxwellian, G = Gaussian.

The analytical situation is complicated by the fact that many of the particle designs are still classified by the governments doing the research so that one can only allude to the problems that may occur by studying very general pellet spectra.

A few words are in order about the reference laser pellet spectra that we will use throughout the rest of this paper. First of all it includes $\sim 20\%$ of the incident light (assumed to be from a CO_2 laser) reflected from the pellet and secondly, it contains 2% of its total energy in 1 keV blackbody (BB) temperature X-rays. It also contains almost 21% of pellet yield in charged particles and there is both a thermalized and fast helium spectrum resulting from the 3·5 MeV α-particles. The particles spectra are represented by either Maxwellian or Gaussian distributions in lieu of more detailed results.

The actual *flux* of the pellet debris to the first wall depends on the energy distributions and the distance over which the particles must travel. To illustrate the complex nature of the flux we have plotted it in fig. 7 for the particles listed in table 1 incident on a spherical first wall 7 m from the pellet (Hunter and Kulcinski 1978 a). Note that the neutrons arrive first, followed by the fast helium ions. The thermalized D, T and He ions begin to arrive before the last of the 'fast' helium spectrum and finally the Si atoms begin to arrive at ~ 2 microseconds from the TN (Thermonuclear) burn. The whole process takes $\sim 10^{-5}$ seconds and then there would be a

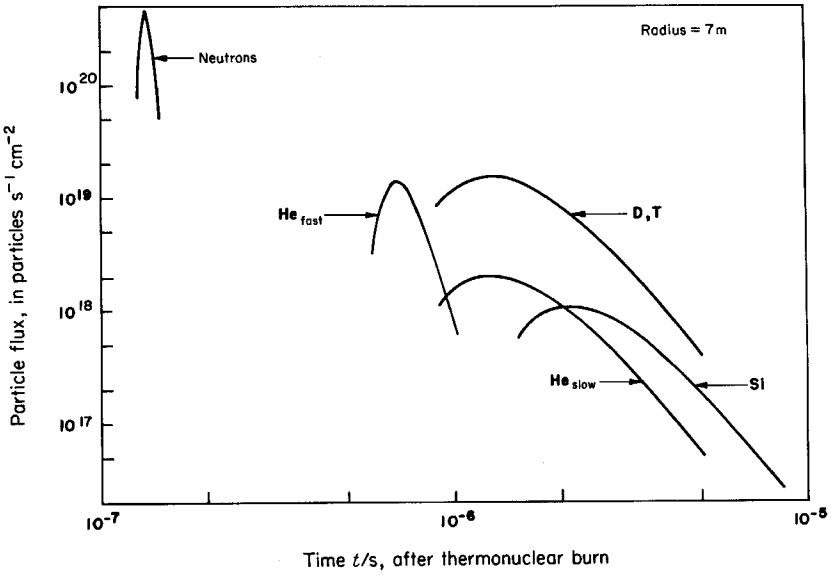

Fig. 7. Particle flux to exposed surface of copper from spectra in table 2.

relatively long time before the next pulse arrives, some 0·1 to 1 second later. Obviously such a complex irradiation schedule is difficult to analyse and only recently have methods been available to treat arbitrary spectra (Hunter and Kulcinski 1978b). Several methods to modify these intense pulses of very high energy ions have been proposed ranging from magnetic fields (Frank *et al.* 1974) to liquid metal films (Booth 1972), gas in the reaction chamber (Conn *et al.* 1977, Hunter and Kulcinski 1978a), and thick sheets of liquid metals (Maniscalco, Meier and Monsler 1977) but none of them have been proved thus far and they all have their own disadvantages.

2.3. *Thermal environment*

The very nature of the DT fusion process requires that essentially all of the energy generated passes through the first wall either in the form of neutrons, or as heat generated by the deposition of photons, charged particles or neutral atoms. Transfer of heat requires that thermal gradients be established and these thermal gradients can induce thermal stresses in rigidly constrained structures.

For a steady state heat flux, the thermal stress level is simply

$$\sigma = \pm \frac{\alpha E}{2k(1-\nu)} \left(W_s + \frac{W_n t}{2} \right) t \qquad (2)$$

where α = thermal expansivity,
E = Young Modulus,
k = thermal conductivity,
ν = Poisson ratio,
W_s = surface heating from energetic particles and photons per cm^{-2},
W_n = nuclear heating per cm^{-3},
t = thickness of wall.

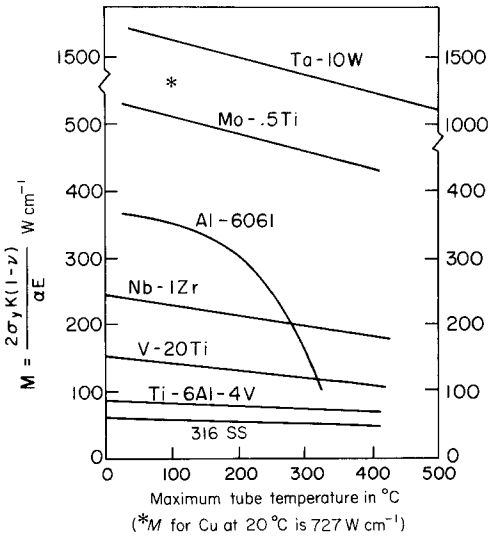

Fig. 8. Thermal stress parameter *vs.* temperature.

The stress in eqn. (2) is found to depend on three general parameters. The first is the combination of materials parameters ($\alpha E/k(1-\nu)$), the second consists of the heating characteristics of the plasma (W_s, W_n) and the third is the thickness of the wall. For fixed wall thickness and plasma conditions we can divide eqn. (2) by the yield strength, σ_y, to obtain a figure of merit which is $[2\sigma_y k(1-\nu)]/\alpha E$†. This is plotted in fig. 8 for various CTR materials (Sze, unpublished results). It can be seen that refractory metal alloys and Al alloys (up to $\sim 200°C$) show the lowest induced stress level. Austenitic steels develop the highest stresses while Ti alloys are somewhat better.

The effect of plasma conditions on the allowable first wall neutron flux limit in 316 SS is shown in fig. 9. Here Sze (1978) has considered 1 mm thick tubes for H_2O and He cooling and 3 mm thick walls for Li cooling. The neutron heating has been kept constant at $10\,W\,cm^{-2}$ per $MW\,m^{-2}$ of neutron wall loading and the allowable neutron wall loadings is expressed as a fraction of the surface heating (in $W\,cm^{-2}$) to the neutron wall loading in $MW\,m^{-2}$. The maximum allowable value of neutron wall loading corresponds to that value which produces a thermal stress equal to the yield stress.

If all the kinetic energy in the 3·5 MeV He atoms were converted to photons or transferred to the neutral atoms, the maximum ratio of surface heat loading to neutron wall loading would be $\sim 20\%$. This corresponds to $P_{max} \sim 2$–$4\,MW\,m^{-2}$ for all three types of cooling systems (P_{max} = total maximum heat flux that the first wall can stand, in $MW\,m^{-2}$.). If, on the other hand we could reduce the fraction of the thermonuclear energy that ends up as surface heat on the first wall to less that 5%, the allowable neutron wall loading would increase to 5–15 $MW\,m^{-2}$. It is very difficult to get the P_s less than 5% of P_n even with the use of divertors and values in

† This is inverted so that large values are desirable.

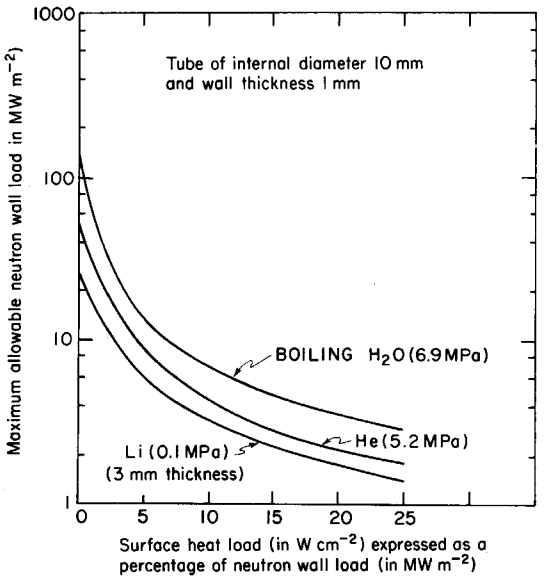

Fig. 9. Maximum heat load to 316 SS tube in fusion plasma environment.

the neighbourhood of 10–15% are not unreasonable for cold gas blanket systems (P_n = neutron wall loading in MW m^{-2}, P_s = surface heat flux due to photons and charged particles, in MW m^{-2}.). This, coupled with the fact that one would probably use a safety factor of ~2 means that thermal stresses will limit the useful neutron wall loadings in 316 SS Tokamak first walls to a few MW m^{-2}. Another study has recently come to the same conclusion (Abdou *et al.* 1977).

The situation with respect to inertial fusion first walls is different in that the heat fluxes are pulsed, and therefore melting (along with the generation of shock waves) becomes a distinct problem. Using the pellet spectra described in table 2 and fig. 7 we can calculate the temperature increase in a 316 stainless steel wall as a function of time after the thermonuclear burn. If we use a radius of 7 m for the first wall we find the temperature increase at the front surface as shown in fig. 10 (McCarville *et al.*, 1978). Note that the X-rays and reflected laser light preheat the surface to over 700 K above ambient for a short period of time (~10^{-9} s) after which the ΔT drops to ~200 K (above ambient) when the fast helium arrives. (The neutrons cause less than 10 K rise and therefore are neglected.) The charged particles greatly increased the surface temperature for 5–10 microseconds with the tritium being most effective. The temperature increase (which is more than sufficient to cause melting) lasts for tens of microseconds and by 1 microsecond after the burn, the temperature is back to within 50 K of the ambient level.

Fig. 10 reveals that unless the steel is operated at a very low temperature, melting would most certainly occur. This problem is better illustrated in fig. 11 where we plot the temperature rise ΔT (for ~1 μs) in 316 SS due to the pellet spectra in table 2 as a function of the distance that the first wall is away from the pellet. Results are shown for 100 MJ and 200 MJ pellets and we have indicated the radius R (and hence the flux) at which the 316 SS will melt if it is operated at an ambient temperature of 325 K. Note that unless the chamber is larger than 8 metre in radius for the 100 MJ

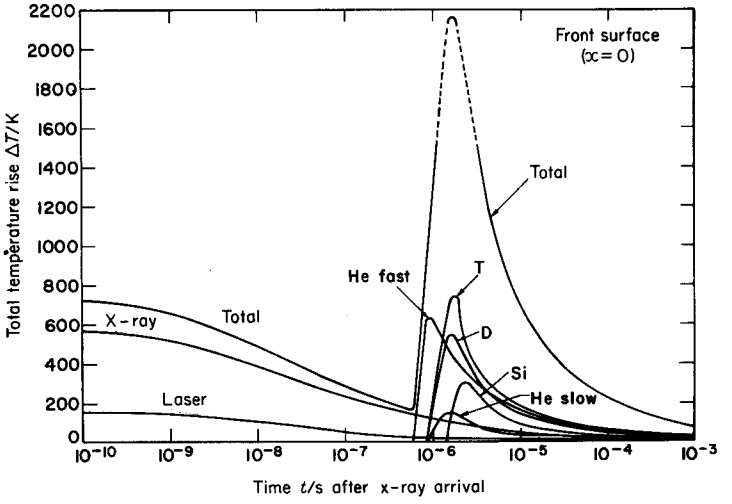

Fig. 10. Thermal response of a 316 stainless steel first wall to pellet spectra from table 2.

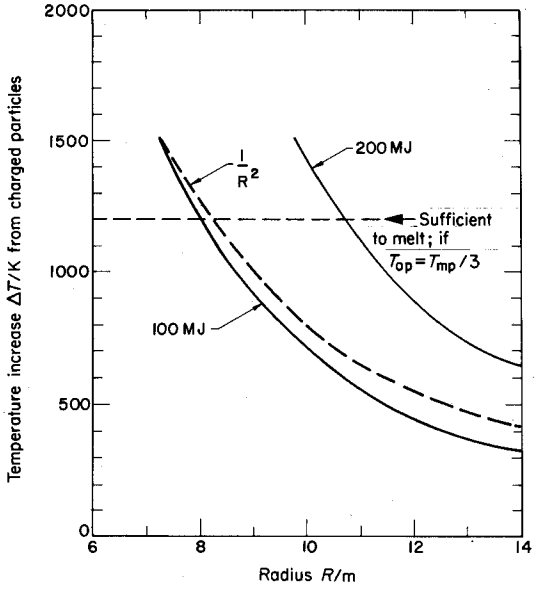

Fig. 11. Temperature increase from pellet debris in table 2.

pellet or 11 metre for the 200 MJ pellet, melting could occur. The fact that the graph of ΔT versus R drops off faster than $1/R^2$ is due to the lowering of the particle flux as the energy spectra of the particles broaden during their flight across the chamber. Fig. 11 graphically illustrates the problem of using higher yield ($\sim$1000 MJ) pellets in stainless steel chambers and it also illustrates the need to find either other first wall materials or ways to modify the pellet debris energy before it impacts on the wall.

Finally, the problem of shock wave generation in laser fusion reactors can be studied with the CHART-D code (Thompson 1973) and a recent analysis shows that

it is only a problem associated with photon fluxes. It is not generally a problem with charged particles because the energy associated with them arrives over such a long time period that it can effectively diffuse away during the pulse (Hunter and Kulcinski 1978a).

Summarizing this section we see that, based on yield strength properties alone, steady state heat fluxes can limit the useful neutron fluxes to the first wall of magnetic confinement systems to as little as a few MW m^{-2} for steel. The nature of the problem is quite different for pellet fusion reactors where melting becomes a formidable problem from 100–200 MJ pellets unless the chamber size approaches unreasonable values, i.e., greater than 15–20 metres in diameter.

3. Primary damage production rates in a fusion reactor environment

Once the neutron and charged particle spectra are known, the production of displaced atoms and transmutation products can be calculated. These two production rates can conveniently be separated for our consideration in this section but, as will be pointed out in the next section, the final disposition of these point defects into two-dimensional or three-dimensional defects depends on the synergistic effects between displaced atoms and transmutants.

3.1. *Displacement of atoms by neutrons*

It is well known that the irradiation of solids with energetic neutrons or atoms can cause some of the atoms of the material to be dislodged from their equilibrium positions and lodged somewhere else in the matrix. The displaced atoms are called interstitials and the 'hole' they leave behind is called a vacancy. The number of such vacancy/interstitial pairs produced per incident particle of energy E per second is related to four important parameters:

Flux of particles of energy E.
Probability, $\sigma(E)$, that the incident particle with energy E will undergo an interaction with a matrix atom.
Probability, $K(E,T)$, that if an interaction takes place, it will produce a primary-knock-on-atom (PKA) with kinetic energy T.
The number of atoms, $\nu(T)$, subsequently displaced by the PKA.

This can be expressed mathematically as, where N_0 is the atomic density,

$$N_d(E) = N_0 \int \phi(E)\sigma(E)K(E,T)\nu(T)\,dT \tag{3}$$

We have already examined the flux of bombarding particles and their characteristic energies in Section 2 and the reader is referred to Evans (1955) for a more complete discussion of the interactions between neutrons and stationary atoms, to Brice (1972) for the interaction between energetic ions and stationary atoms, and to Doran *et al.* (1973) for a description of the secondary displacement models with PKA's of kinetic energy T. For the rest of this section we will concentrate mainly on the production of damage by neutrons. This damage is more uniformly spread throughout the structure than the surface damage produced by the energetic atoms from the plasma.

The interactions of a neutron with an atom (and hence the production of displaced atoms) can occur via many mechanisms. For example, it could occur via an elastic reaction where kinetic energy is conserved or by an inelastic reaction where the struck atom is left in an excited state. In the latter case, the nucleus can dispose of

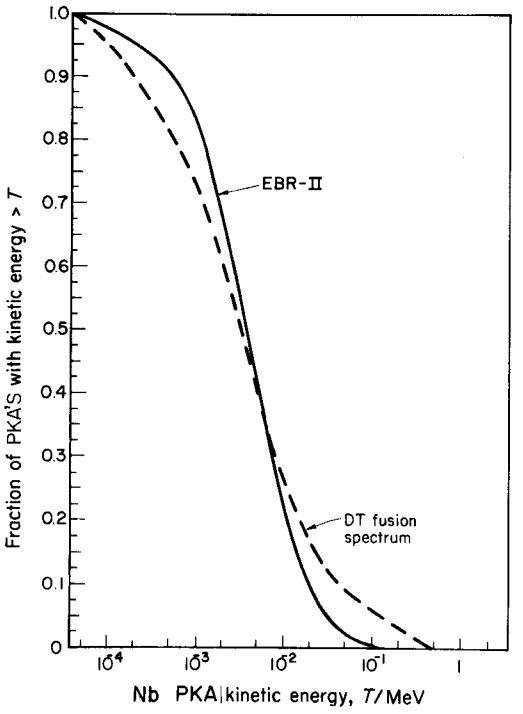

Fig. 12. Comparison of niobium fractional PKA distributions in various neutron spectra.

this excitation energy by emitting a gamma ray, one or sometimes two neutrons, or it can decay by emitting charged particles such as hydrogen or helium ions. Following the emission of the extra particles, the original nucleus can recoil with sufficient energy to cause many more displacements. In fission reactors, the neutron energy is low enough so that only the elastic reactions are of any importance. However, in fusion reactors, the higher energy neutrons can promote many inelastic reactions such as (n, n'), (n, 2n), (n, p), (n, α), etc.

The resulting PKA's from irradiation in the two types of nuclear facilities can be quite different. Fig. 12 shows the kind of PKA spectra to be found in Nb irradiated in the core of EBR-II, or by a typical fusion neutron spectrum (see Avci, to be published). Note that the number of PKA's at very low energies is greater in a fission spectrum than in a fusion spectrum and vice-versa at high energies. At high energies, the increased PKA energy results mainly from the recoils produced by charged particle emission reactions although the elastic reactions with 14 MeV neutrons do make some contribution.

Once the PKA spectrum is established, the resulting number of atoms displaced by a neutron of energy E can be calculated from appropriate displacement models. The result can be placed in the form of a total displacement cross section, $\sigma_d(E)$, which sums up the contribution from the various nuclear reactions. The product of this cross section with the neutron fluence, $\phi(E)t$, is commonly given in units of dpa which stands for *displacement per atom* and represents the fraction of the matrix atoms which have been displaced during the time period t. Such a unit allows one to compare quite different irradiation environments such as fission reactors to fusion

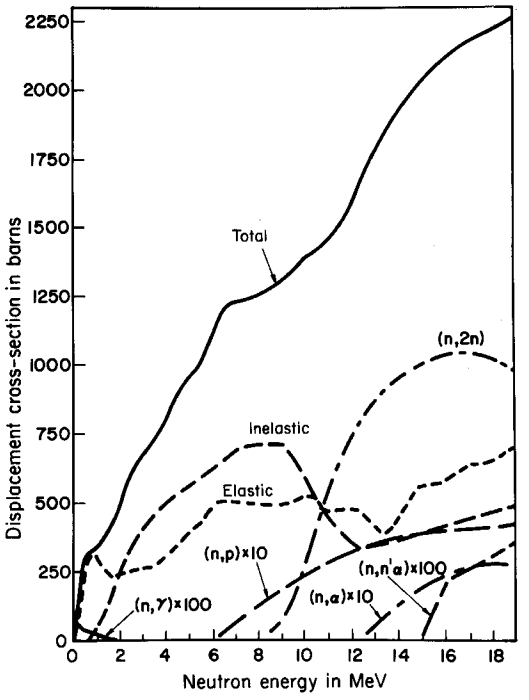

Fig. 13. Individual contributions to the total niobium displacement cross-section.

reactors, and relate to results obtained from electron irradiation, or even from heavy ion bombardment. However the dpa unit does not account for rate effects, recombination of vacancies in the cascade region or spatial rearrangements due to thermally assisted migration. Nevertheless, it is a useful unit to compare first order effects that might be expected in various irradiation environments.

Returning to eqn. (3) we find we can calculate the individual displacement cross sections from the various nuclear interactions by

$$\sigma_d^i(E) = \int \sigma^i(E) K(E,T) \nu(T)\, dT \tag{4}$$

where $\sigma^i(E)$ is the neutron interaction cross section with the lattice atoms for the ith reaction.

An example of the individual cross sections for Nb as well as the total displacement cross section is shown in fig. 13 (Avci, to be published, Odette and Doiron 1976). Seven contributions have been included; (n, γ), elastic scattering, (n, n), (n, p), (n, α), (n, 2n), and (n, n'α). It can be seen from fig. 13 that there are three dominating reactions: 0–2 MeV, elastic scattering; 2–10 MeV, inelastic scattering (n, n'); 10–20 MeV, (n, 2n) reactions. The above information reveals that, in contrast to fission reactors where most of the atoms are displaced by elastic scattering reactions, the majority of the atoms in a fusion reactor Nb first wall will be displaced by the recoil from the (n, 2n) reaction. This will have an impact on the PKA spectra as we saw in fig. 12.

Another important point to note is that the total displacement cross section is not linear with neutron energy. For example the value of σ_d 14 MeV/σ_d 1 MeV is not 14

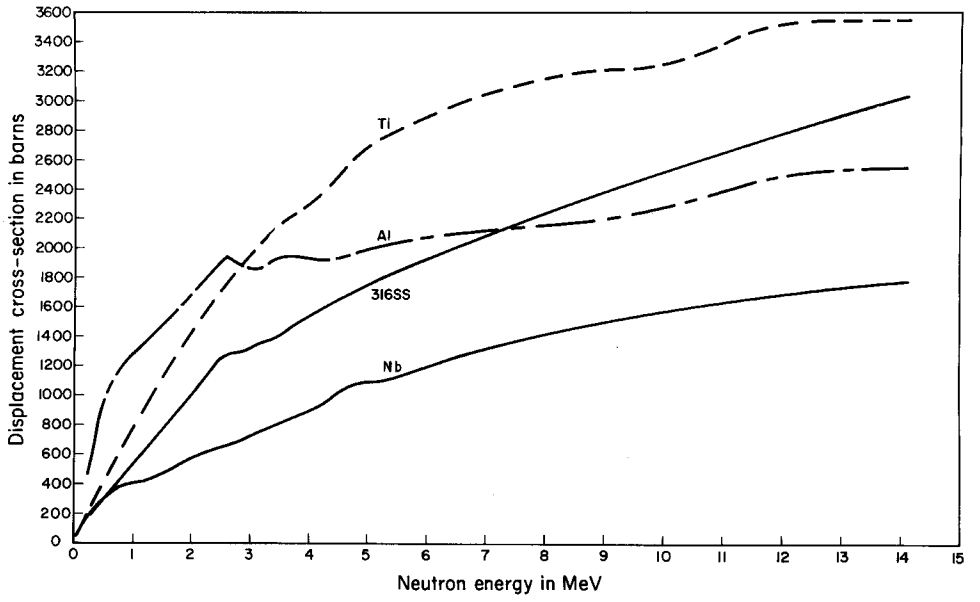

Fig. 14. Neutron displacement cross-sections for various materials.

but more of the order of 4 to 6 for heavy elements such as niobium and the alloy 316 SS, while it is only ~ 2 for light elements like aluminium (see fig. 14). Much more of the kinetic energy of the PKA's from the higher energy reactions in aluminium appear as electronic excitation (heat) rather than in atomic displacements.

Armed with the values of σ_d for all the potential first wall materials and first wall neutron fluxes one can calculate the displacement rates in various first wall configurations. A representative set of values is shown in table 3. Note that the dpa rates are similar, varying by only a factor of two from niobium to aluminium. However, the reader should be cautioned that raw displacement numbers alone are not sufficient to judge the final performance of materials, other factors such as the damage rate, PKA spectra, temperature and stress must also be considered.

The next important topic to consider is the instantaneous rate at which the damage is produced in the first wall. The typical variations that can occur in just one material for various types of nuclear facilities are shown in table 4. Data are included for magnetic and inertial confinement systems as well as for fast and thermal fission reactors, neutron test facilities, and simulation facilities such as heavy ion and electron accelerators. It can be seen from table 4 that the displacement rates in a Tokamak or Mirror reactor are comparable or even lower than presently achievable in fission reactors. This is true up to wall loadings of $\sim 3\,\mathrm{MW\,m^{-2}}$. Simulation facilities can produce much higher displacement rates than those found in either fission or fusion reactors. While present 14 MeV facilities produce damage rates somewhat lower than expected in quasi-steady state fusion systems, future D-Li spallation neutron facilities will produce dpa rates equivalent to $\sim 10\,\mathrm{MW\,m^{-2}}$ in a small volume.

There is one more important point in table 4 and that is the extremely high dpa rate produced by the bursts of neutrons from the imploded pellets of inertial fusion facilities. Damage rates of 3 dpa per second can occur for $\sim 10^{-7}$ s per $\mathrm{MW\,m^{-2}}$. Of

Table 3. Summary of the yearly averaged reaction rates in typical fusion reactor first walls (Kulcinski, Abdou and Doran 1975, Gabriel, Bishop and Wiffen 1978).

Material	dpa/yr†	appm He/yr		appm H/yr†
		Fusion†	EBRII	
316 SS	6·8	105	13·8	374
V	8·1	39·6	0·88	172
Nb	5·1	16·7	1·51	73
Mo	5·7	33·0	1·78	47
Al	11·9	223	16·3	208
Ti	11·1	73·7	3·73	109

†70% capacity factor, 1 MW m^{-2}.

Table 4. Summary of instantaneous displacement rates in a 316 SS first wall and other irradiation test facilities.

System	dpa per second	Note
Fusion:-		
Tokamak or Mirror	3×10^{-7}	1 MW m^{-2}
Laser	~3	For 10^{-7} s, 1 MW m^{-2}, 1 shot per second (neutrons only)
Fission:-		
EBR-II	$\sim 10^{-6}$	62·5 MW, core centre
HFIR	$\sim 10^{-6}$	100 MW, core centre
Neutron test facilities:-		
RTNS-II	5×10^{-8}	2×10^{13} n cm^{-2} s^{-1}, 1 cm^3 volume
FMIT	3×10^{-6}	Operational in 1983; 10 cm^3 volume
Simulation facilities:-		
Heavy ions	10^{-4} to 10^{-2}	0·01 to 1 μA cm^{-2}, 20 MeV Ni
Electrons	10^{-3}	Typical 1 MW high voltage electron microscope

course the dpa rate averaged over the associated period of one shot is approximately the same as for a magnetically confined plasma system. Recent studies of the point defect kinetics reveal that quite a few less vacancies and interstitials may be left after such high production rates compared to the production of the same number of defects over a much longer time period (Ghoniem and Kulcinski, to be published). The lack of test facilities to confirm these predictions is a major roadblock to a true assessment of the problems such high damage rates might impose.

3.2. *Transmutation rates*

In addition to the normal (n, γ) reactions which cause some elements to be transmuted to others, the higher energy neutrons of a fusion reactor can produce gaseous atoms via (n, p) and (n, α) reactions. Of the two types of transmutant atoms, solid or gaseous, it has been generally observed that gaseous atoms can have the greater effect on the mechanical behaviour of a metallic system. This is not to say that the production of elements like Zr in Nb or Mg in Al can be neglected, because in some systems the metallic transmutants are very important. However, it has been noticed that only a few atomic parts per million of helium (appm He) in 316 SS at elevated temperatures can produce a very large degradation in the mechanical

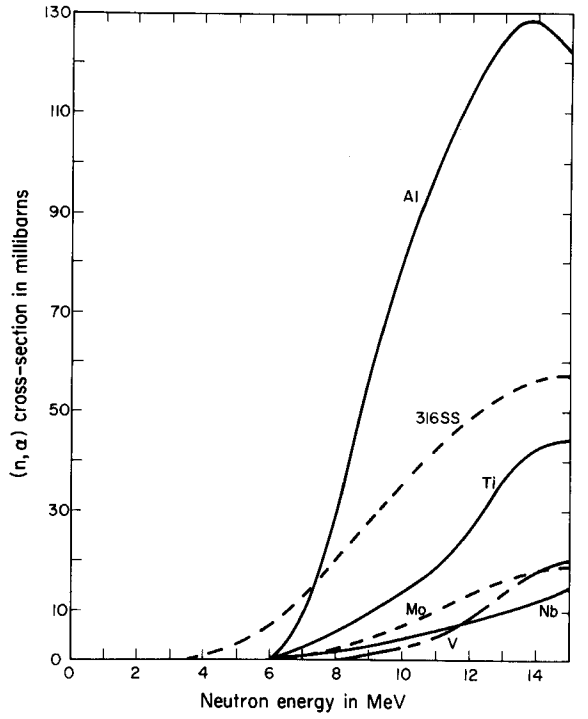

Figure 15. Helium gas production cross-section.

properties (Kramer *et al.* 1968, Bloom and Wiffen 1975). We will come back to this point in Section 4 but for the remainder of this section we will concentrate on the gaseous impurities.

Perhaps the best way to understand why the production of helium atoms in a fusion spectrum is so much larger than that in a fission spectrum is to examine the energy dependence of the (n, α) cross section. The total helium production cross sections for Al, V, 316 SS, Nb, Ti, and Mo are plotted in fig. 15 as a function of neutron energy. Note that in the 1–2 MeV region, where most of the neutrons are born in a fission reactor, the gas production cross sections are low, hence the low He production rate (see also table 3). However the helium production cross sections are 100 to 1000 times higher in the 14 MeV region and hence the helium production rates in fusion reactors will be an order of magnitude larger than in fission facilities. The same sort of cross-sectional dependence is typical of hydrogen production.

3.3. *Ratio of transmutation to displacement rates by neutrons*

One of the most convenient parameters that can be used to characterize neutron spectra is the ratio of transmutation rates to displacement rates. Such a number is independent of the neutron flux and is very sensitive to subtle changes in the backscattered spectra.

Typical appm He/dpa ratios are given in table 5 for potential CTR materials in both fission and fusion environments. The first point to notice is the fact that the ratios are much higher (by one to three orders of magnitude) for fusion environments than for fission systems. The second point is that there is one major exception to the

Table 5. Typical helium-production to displacement-damage ratios for fusion materials (Kulcinski, Abdou and Doran 1975, Gabriel, Bishop and Wiffen 1978).

Material	(appm He)/dpa	
	Fusion	Fission (EBRII)
316 SS	15·4	0·63†
V	4·9	0·03
Nb	3·3	0·09
Mo	5·8	0·10
Al	18·7	0·31
Ti	6·6	0·11

†For a thermal reactor like HFIR, this ratio is much higher because of the $^{58}Ni(n,\gamma)^{59}Ni(n,\alpha)^{56}Fe$ reaction. Values as high as 60 to 70 have been achieved.

previous observation and that is the helium to dpa ratio in Ni containing materials irradiated with thermal neutrons. This unique situation arises from the $^{58}Ni(n,\gamma)^{59}Ni(n,\alpha)^{56}Fe$ double capture sequence. Since neither fast fission nor fusion reactors contain many thermal neutrons, this sequence is not important in those systems. Scientists have been able to capitalize on this quirk of nature by irradiating nickel-containing alloys in thermal fission reactors to achieve appm He/dpa ratios typical of fusion reactor spectra (~ 15) or even as high as a ratio of 60 to 70 (Bloom and Wiffen 1975).

Finally, the data in tables 3, 4 and 5 show that, aside from the unique case for nickel-containing alloys in a thermal neutron environment, there is presently no neutron test facility that can produce the 'correct' ratio of gas atoms to displaced atoms at a sufficient damage rate to achieve even a few months of anticipated operation. This means that we really have very little data upon which to make a judgement of materials performance.

3.4. *Displacement damage due to charged particle pellet debris in laser fusion reactors*

One problem that is unique to the inertial confinement fusion reactors is the high flux of energetic particle debris that comes from the exploding pellet. In general, the energy and variety of the particles is greater than in the magnetic confinement systems. The energies may range from tens of keV to MeV and the damage may extend several micrometres into the surface. The fact that the pellet debris is not monoenergetic means that the particles will arrive at the first wall at different times (fig. 7) thus making an extremely complex spatial and temporal analysis necessary. The situation has been recently analysed in a series of papers (Hunter and Kulcinski 1978 c) and we will quote only some of the more interesting results here.

Following the approach in Section 2.2, the reference spectra in table 2 and the fluxes from fig. 7 we have calculated the displacement rates in a copper first wall some 7 metres from the imploding pellet. The copper could be representative of the last focusing mirror facing the pellet, but analyses for 316 Stainless Steel (McCarville *et al.*, 1978) and for molybdenum (Hunter and Kulcinski, 1978 d) have also been performed. The resulting displacement rates at the surface ($x=0$) are plotted in fig. 16 and it is noticed that the first displacements in this system result from the neutrons which arrive some 10^{-7} s after the pellet burn. These neutrons produce displacement rates of $\sim 4\,\text{dpa}\,\text{s}^{-1}$ about $0{\cdot}5\,\mu$s before the next wave of damage

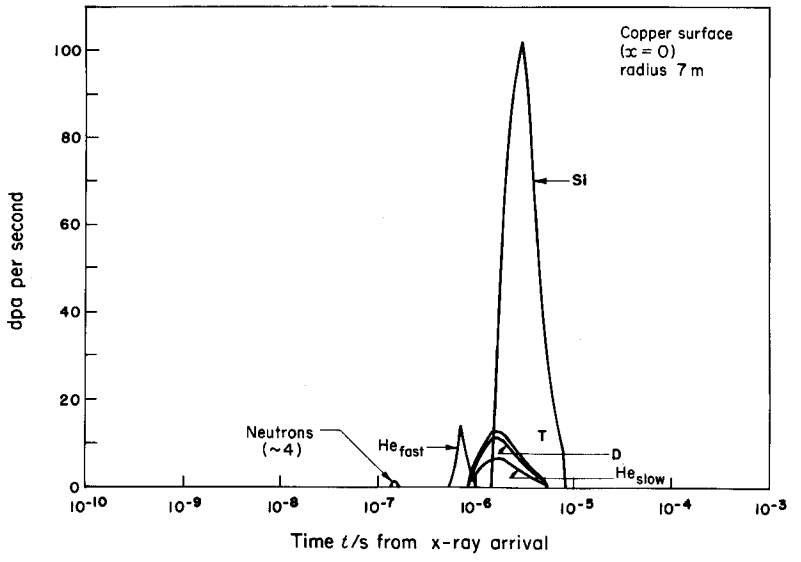

Fig. 16. Component displacement rate in copper from pellet debris in table 2.

particles arrive. The energetic helium atoms then produce damage of up to $15\,\mathrm{dpa\,s^{-1}}$ for $\sim 0{\cdot}5\,\mu\mathrm{s}$. The thermalized D, T and He atoms then produce $10\text{–}20\,\mathrm{dpa\,s^{-1}}$ each for the next $5\,\mu\mathrm{s}$. While the lighter particles are producing damage, the silicon atoms arrive producing damage rates up to $100\,\mathrm{dpa\,s^{-1}}$ for $\sim 8\,\mu\mathrm{s}$. If the same analysis is done at $1\,\mu\mathrm{m}$ from the front surface, near the end-of-range for the energetic silicon atoms, the total dpa rates can approach $500\,\mathrm{dpa\,s^{-1}}$ for a few microseconds!

The important point of the above analysis is that the instantaneous damage rates can be very high, as much as a factor of 10^8 over present nuclear fission facilities (fig. 17). We have no experience with such damage rates experimentally and only recently have theories of radiation damage been modified to consider the effect of such high dpa rates on processes like void growth (Ghonien and Kulcinski 1978). It is also important to note that there will most likely be some synergistic efforts between the high temperatures generated in first walls of inertial confinement systems (Section 2.3) and the high dpa rates. This is illustrated in fig. 18 where the temperature and displacement rates are superimposed on the same graph for the pellet spectra of table 2. It is noticed that some very high temperatures preheat the first wall before the pellet debris arrive. This can have a large effect on processes like sputtering which have been shown by Nelson *et al.* (1965) to be sensitive to temperature. In fact, it has been shown by Hunter and Kulcinski (1978a) that the erosion rate could be increased by a factor of 4 over that which might be incurred if no preheating of the surface took place. Finally, even though these extremely high temperature and displacement transients only take place within the first few micrometres of the surface, one must consider carefully the effect that they will have on processes such as void or bubble growth, blistering or the initiation of microcracks which could severely reduce the fatigue life.

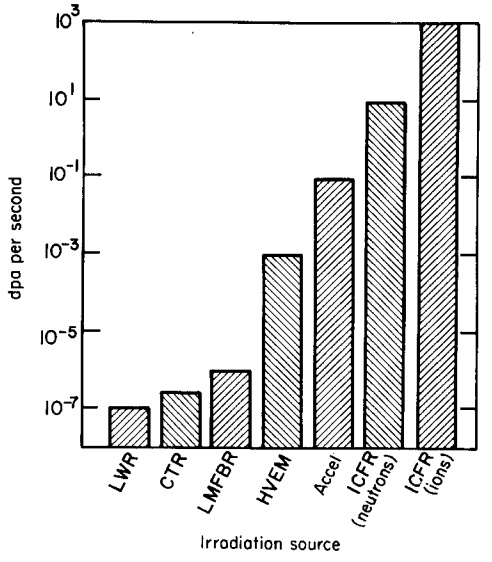

Fig. 17. Comparison of peak damage rates in various nuclear facilities.

Key to legends: LWR—Light Water Reactor; CTR—Controlled Thermonuclear Reactor; LMFBR—Liquid Metal Fast Breeder Reactor; HVEM—High Voltage Electron Microscope; ACCEL—Heavy Ion Accelerator; ICFR—Inertial Confinement Fusion Reactor.

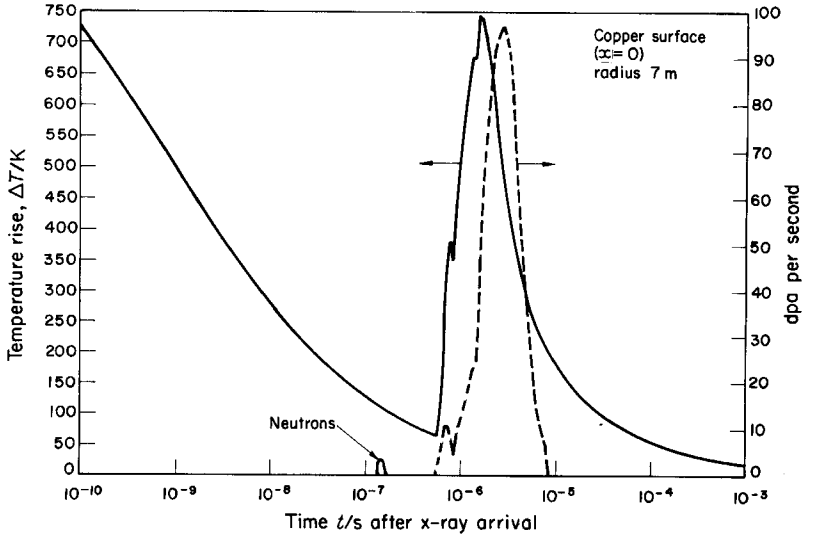

Fig. 18. Temperature rise and displacement rate in copper from pellet debris in table 2.

4. Possible materials responses to primary damage rates in fusion reactor first walls

4.1. *General features*

Once the radiation environments and primary defect production rates are well established, the next question is, "How will the materials in the first walls accommodate to these damage conditions?". On the basis of our past experience with fission reactor environments we can estimate what *might* happen but it should be remembered that we have not yet irradiated any material to even 0·1% of the yearly anticipated damage levels in the environment of a DT plasma.

Of the possible secondary responses to the damage outlined in fig. 1, two stand out as potential barriers to long useful lifetimes. These are swelling of the metallic structures due to the formation of voids and loss of ductility. We will come back to these two later. The other mechanisms, such as wall erosion due to sputtering and blistering have implications on the plasma performance as well as on the first wall performance. However, the actual removal rates are very design dependent. This area has been the subject of many conferences (see Wiedersich *et al.* 1974, Bauer *et al.* 1976) and the reader is referred to Kaminsky (1965, 1976) for a thorough discussion of the phenomena involved.

The production of solid transmutation products which subsequently decay radioactively and generate heat was recognized as a problem very early in the assessment of fusion materials (Vogelsang *et al.* 1974). While this phenomenon has some environmental implications and, in some materials, rather substantial chemical changes can take place (e.g., Zr in Nb or Mg or Al), other factors have limited the useful lifetime to the point where chemical changes are rather small at the anticipated time of replacement.

It is well known from fission reactor experience that when metals are irradiated with neutrons at the same time that they are subjected to high temperatures and stresses, the creep rate can be substantially increased (Gilbert *et al.* 1972). There is every reason to believe that such an effect will also be observed in fusion reactors but unlike the situation in fission reactor cores, the anticipated dimensional tolerances will be considerably larger in the first wall and blanket structure. In fact, the relaxation of stresses induced by manufacturing defects, differential swelling, and thermal gradients may even reduce the potential for failures in the event of unscheduled power excursions. Since the assessment of creep rate effects is also very dependent on design features—the method of cooling (low pressure liquid metals or high pressure gas), the thickness of the first wall coolant channels, and so on, it is not an area that can be properly estimated at this time. As the field progresses, it will certainly be necessary to reassess the importance of this phenomenon to the overall performance of the first wall.

Finally, the necessity for maintaining very good vacuum conditions in most magnetic fusion devices means that particular attention will have to be paid to the prevention of cracks that may form in the welds and the portions of the first walls which contain the high pressure coolants. Even small leaks, of the order of one per 1000 square metres, could shut down a large fusion reactor. The production and propagation of small cracks in potential fusion first walls has been discussed by Abdou *et al.* (1977) and Mattas and Smith (1978) and they have shown that in one of the earlier reactor designs, UWMAK-I, the propagation of an initial 0·1 mm deep crack could limit the wall life to less than two years at 1·25 MW m^{-2}. Such a

prediction is indeed serious and it points out that quality assurance procedures will have to be quite extensive to prevent such a limitation from occurring. However, the crack propagation rates are very sensitive to the plasma dynamics (that is, the burn time and the 'down time' between burns') and it is too soon to make general statements about the final limiting features.

This brings us back to the two major problems that have been identified for fusion reactor first walls and we will treat them separately.

4.2. *Swelling*

We have now had ten years of experience in dealing with the production of voids in metals by neutron irradiation. Since the first voids were observed in steel by Cawthorne and Fulton in 1966 voids have been observed in over a dozen elements (Mg, Al, V, Fe, Co, Ni, Cu, Nb, Mo, Ta, W, Re and Pt) and scores of alloys. The general conditions under which voids are formed seem to be well known. For example, it is known that voids only form at temperatures above which the vacancies are mobile (usually, above 30% of the melting point) and it appears that some form of nucleating agent such as gas atoms is required for the stabilization of the void embryo. It is also known that voids do not grow at very high temperatures (above $\sim$50% of the melting point) because the vacancy supersaturation is not sufficient to keep the voids from evaporating. Once an incubation period has been passed, the swelling appears to be roughly linear with damage level. It is also apparent that high stresses can enhance void growth rates and the addition of helium will enhance the nucleation rates. The nucleation and growth of voids is also very dependent on the rate at which the damage is produced; the higher the damage rate, the higher the temperature must be for a similar amount of void swelling. Finally, the effect of impurities and prior thermo-mechanical treatment is also very pronounced and in general, the more impure the material, the longer the incubation period before the voids are nucleated and begin to grow. The reader is referred to Corbett and Ianniello (1972), Matthews (1977), and a recent conference edited by Nelson (1975) for more general information on void production in metals.

The overall effect of the production of voids in metals is that the material will expand and possibly distort rigidly held components, thereby raising the stresses and promoting early failure. The fact that the first wall of a fusion reactor will be simultaneously subjected to damage, temperature and stress gradients, means that the swelling will not be uniform and consequently local swelling gradients will be established.

The unique features of the fusion reactor environment that make the void production phenomena somewhat different from those in fission reactors are,

higher helium and hydrogen gas production rates (Section 3.2),
lower damage rates in magnetically confined systems and much higher damage rates in inertial confinement approaches (Section 3.1),
the PKA differences between 14 and 1 MeV neutrons (Section 3.1).

At the present time there are no *experimental* data which would indicate that under identical conditions (i.e., temperature, stress, dpa rate) irradiation with 14 MeV neutrons will be more or less effective than fission neutrons in promoting void swelling. It is well-known that the average PKA energy is much higher than in the case of fission reactors and one might expect that the larger displacement cascades would promote higher recombination rates, thereby leaving fewer vacancies

available for the voids to grow. However, such a possibility may be offset by a more efficient nucleation rate because of the higher helium generation rate so that the end result is not clear.

The damage rates in fission reactors are only slightly above those anticipated in most magnetically confined fusion reactor conceptual designs so we might expect to first order, no substantial change in the temperature range over which the voids might form. On the other hand, the extremely high dpa rates of the inertial confinement systems will most certainly affect the number of free defects available for void growth. Ghoniem (to be published) has shown, theoretically, that the higher dpa rates will reduce the void growth rate and coupled with the extremely high temperature pulses associated with laser fusion first walls (Hunter and Kulcinski, 1978 c), significant annealing could take place between shots. Whether or not this happens in experiments remains to be seen, but the sheer magnitude of the difference in displacement rates (over 10^8 from our present fission reactors and 10^5 over current heavy ion simulation studies) makes behaviour similar to fission reactor irradiation very unlikely.

Finally, the effect of large amounts of helium during irradiation is likely to increase the amount of swelling especially at high temperatures. Experiments by Maziasz *et al.* (1976) have shown that when large amounts of helium (greater than a 1000 appm He) are added during irradiation via the nickel-58 double capture sequence in thermal reactors (Section 3.2), the swelling is substantially higher than in the same material irradiated in EBR-II (see fig. 19). This enhanced swelling is probably due to increased nucleation rates and the formation of helium bubbles which do not evaporate at high temperatures but, in fact, grow.

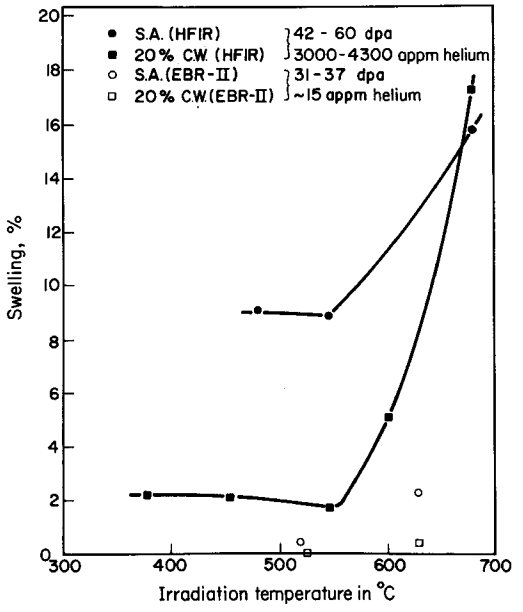

Fig. 19. Swelling in 316 SS irradiated in fast (EBR-II) and thermal (HFIR) reactors.

Key to legends: HFIR—High Flux Isotope Reactor; EBR-II—Experimental Breeder Reactor-II; S.A.—Solution Annealed; C.W.—Cold Worked.

In summary, it is expected that voids will continue to be a problem for magnetic confinement fusion reactor first walls just as they have been a problem for the cladding in fast fission reactors. The situation is not as clear in inertial confinement systems and there is an urgent need for some definitive experiments. The fact is that up to the present time, no voids have yet been produced by 14 MeV neutrons because there are no facilities capable of producing high enough neutron fluxes.

4.3. *Ductility effects*

An even more serious problem than swelling is found when one examines the possible effects of 14 MeV neutron irradiation on the ductility of potential fusion materials. First of all, a certain amount of ductility is necessary in any large structure in order to provide relief for the consequences of all manufacturing defects, unanticipated temperature and stress excursions and continually changing materials properties, as the reactor is operated. In the extreme case, where there is no ductility available, any stress which exceeds the yield strength would cause a component to fracture with catastrophic results in a large, highly radioactive structure containing hundreds of millions of curies of tritium and activated materials. Obviously, one needs to have some capability of plastic deformation as a protection.

Current design philosophy in the LMFBR programme for the fuel cladding is that at least 0·5% uniform elongation should be available beyond the yield point. Since the LMFBR can operate with a few failed elements, whereas a fusion reactor probably cannot operate with as much as one major leak, it is quite possible that even higher levels of ductility will be required. No determination of that number can be made at this early stage of consideration but it is the author's opinion that at least a 1% level of uniform elongation will be required for safe operation.

The loss of ductility of metals is tied to at least three mechanisms; production of high densities of dislocation loops, formation of second phase precipitates, and helium gas bubble formation. Of the three mechanisms, the latter is perhaps the most serious. It has been shown that helium levels of as little as 10 appm can reduce the uniform elongation in stainless steel to well below the desired level of 1% at temperatures above 500°C (Fish *et al.* 1973). The mechanism of this degradation is fairly simple. The helium gas migrates to or is swept up by moving grain boundaries and bubbles are formed at the interface between two grains (fig. 20). The interiors of the grains are hardened by the formation of dislocation loops or voids and any deformation required by the material must be taken up by the grain boundaries. However, as the grain boundaries try to take up the strain, the bubbles act as crack nuclei and the material will fail in a brittle, intergranular fashion. The effect is more pronounced at higher temperatures and recent work by Bloom and Wiffen (1975) shows that above 500°C, the residual ductilities are very low indeed in 316 SS (fig. 21). Also plotted in fig. 21 is the swelling accompanying the loss in ductility which shows that above 500°C, the swelling also becomes rather large because of the growth of the helium-filled bubbles.

The high production rates of helium in all materials considered for fusion first walls makes the above observations particularly disturbing. Unless methods are found to reduce this phenomenon, fusion reactor wall temperatures will have to be reduced to much lower values than those indicated by strength considerations, thereby affecting the economic performance. Two such reactor designs have already moved in that direction. (Conn *et al.* 1978, Steiner *et al.* 1977).

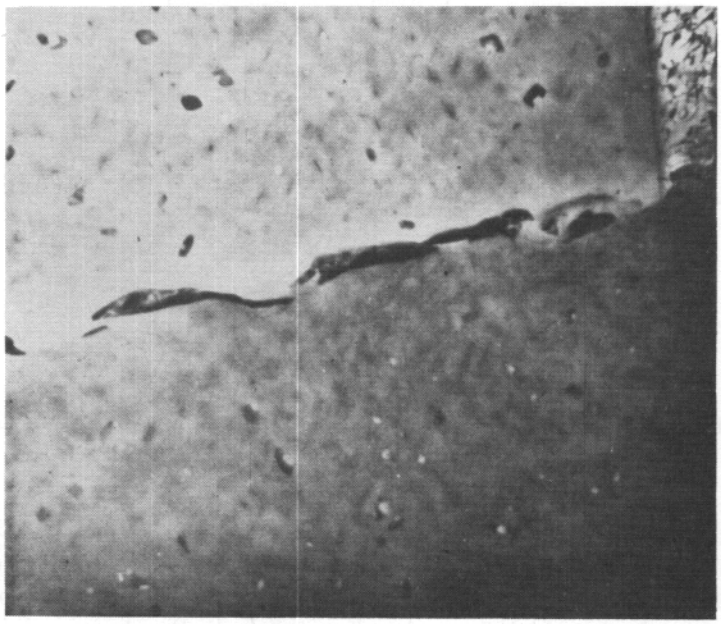

(a)

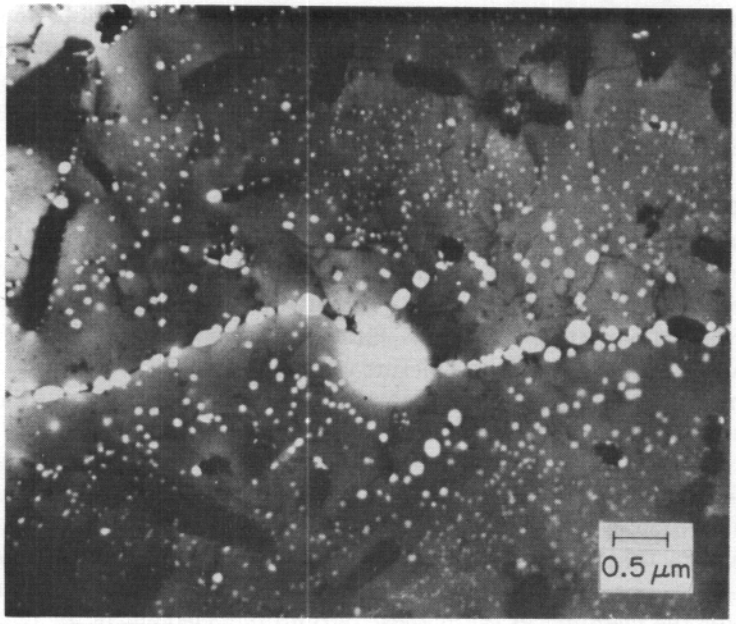

(b)

Fig. 20. (*a*) Irradiated in EBR-II at 580°C to $1{\cdot}9 \times 10^{22}$n cm^{-2} (26 dpa, 5 appm helium). (*b*) Irradiated in HFIR at 575°C to $4{\cdot}2 \times 10^{22}$n cm^{-2} (58 dpa, 1790 appm helium). Wiffen and Bloom, ORNL 1974.)

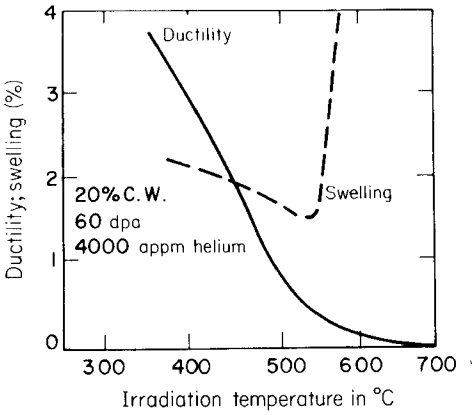

Fig. 21. Effect of irradiation temperature on ductility and void-induced swelling in 316 stainless steel.

Since the production of helium is a nuclear phenomenon characteristic of all the potential CTR materials, the only way to alleviate this effect is to reduce the energies of the neutron spectra, and several approaches to that end have been recently investigated by Avci *et al.* (1978, and to be published). By placing solid or liquid materials between the plasma and first wall the helium production rates can be lowered by two to three orders of magnitude.

In summary, perhaps the most serious characteristics of the DT fusion irradiation environment is the production of large amounts of helium and the subsequent effect it can have at high temperatures on ductility. Experiments in fission reactors with Ni-containing alloys show that steels will have to be limited to 500°C or less because of this phenomenon thus limiting the thermal efficiency of the fusion reactor to less than present LMFBR's†.

5. Concluding remarks

This has been a brief review of a highly dynamic field. It has only been developed in the last five years and is hampered by the lack of suitable testing facilities. The environment of a DT fusion reactor is quite different from those found in present fission or charged particle simulation facilities and therefore we have only begun to define what might be expected. The picture will become much clearer in the next five to ten years as we find which of the present approaches to fusion is most attractive from a commercial aspect.

The job for the materials scientist is just beginning and is even more demanding than the one required by the introduction of fission reactors. It would be desirable to design fusion reactors so that they would last the lifetime of the plant. At the present time this means that the first walls would be required to last for the order of 100 megawatt-years per square metre (which is six times the highest damage level projected for the cladding in the highest burnup fuel element of an LMFBR). A recent paper by this author (1977) summarized how well we are doing in this regard and fig. 22 is taken from that study. We can see that estimated first wall lifetimes for

† Liquid Metal Fast Breeder Reactors.

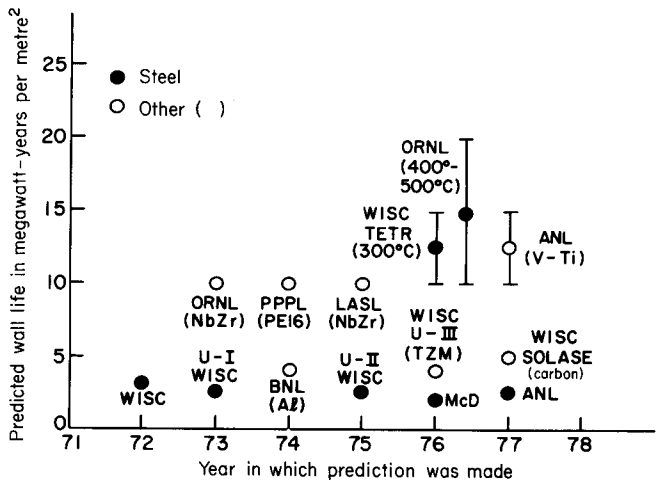

Fig. 22. Predicted first wall life for various reactor designs.

Key to legends:

WISC—Wisconsin
ORNL—Oak Ridge National Laboratory
U-I—UWMAK-I (Wisconsin)
PPPL—Princeton Plasma Physics Laboratory
BNL—Brookhaven National Laboratory
LASL—Los Alamos Scientific Laboratory
U-II—UWMAK-II (Wisconsin)
TETR—Tokamak Engineering Test Reactor
U-III—UWMAK-III (Wisconsin)
McD—McDonnell Douglas
ANL—Argonne National Laboratory
TZM—A molybdenum alloy
PE-16—A nickel-based alloy

steel range from 2–3 MW y m^{-2} at 500°C to as high as 10 or 20 MW y m^{-2} at 300–400°C. These values are far from those desired and have yet to be truly substantiated in a realistic fusion environment.

It should now be apparent why successful control of a fusion plasma in the next five years will be only the start of a very interesting, difficult, and challenging research effort for the materials scientist.

References

Abdou, M. A., *et al.*, 1977, *The Establishment of Alloy Development Goals Important to the Commercialization of Tokamak-Based Fusion Reactors*, Argonne Nat. Lab. ANL/FPP/TM-99.

Aranchuk, L. E., *et al.*, 1978, Studies of inertial confinement electron beam driven thermonuclear fusion, *7th Int. Conf. on Plasma Physics and Controlled Nuclear Fusion Research, Innsbruck, Austria* (Vienna: IAEA) (to be published).

Avci, H. I., *Radiation Effects*, (to be published).

Avci, H. I., Gohar, Y., Sung, T. Y., Kulcinski, G. L., and Maynard, C. W., 1978, *Nucl. Engr. Desi. Engr.*, **45**, 285.

Avci, H. I., and Kulcinski, G. L., *Nucl. Tech.* (to be published).

Badger, B., *et al.*, 1973, *Wisconsin Tokamak Reactor Design—UWMAK-I*, University of Wisconsin Report 68, Vol. I & II.

Badger, B., *et al.*, 1975, *UWMAK-II—A Conceptual Tokamak Power Reactor Design*, University of Wisconsin Report UWFDM-112.

Badger, B., *et al.*, 1976, *UWMAK-III, A Noncircular Power Reactor, Univ. of Wisconsin* Report-150.

BAUER, W., FINFGELD, C. R., KAMINSKY, M., eds., 1976, Surface effects in controlled fusion devices, *J. Nuclear Mat.*, **63.**

BERANEK, F., 1978, Ph.D. Thesis, Univ. of Wisconsin.

BLOOM, E. E., 1972, *Irradiation Embrittlement and Creep* (British Nuclear Energy Society), p. 93.

BLOOM, E. E., WIFFEN, F. W., 1975, *J. nucl. Mater.*, **58,** 171.

BOOTH, L. A., 1972, *Central Station Power Generation by Laser-Driven Fusion*, Los Alamos Laboratory Report, LA-4858.

BRICE, D. K., 1972, *Physical Review* A, **6,** 1791.

CAWTHORNE, C., and FULTON, E. J., 1966, *Nature, Lond.*, **216,** 575.

CONN, R. W., 1978, *J. nucl. Mater.*, **76/77,** 103.

CONN, R. W., *et al.*, 1977, *Solase—A Commercial Laser Fusion Reactor Design*, Univ. of Wisconsin Report, UWFDM-220.

CONN, R. W., and KESNER, J., 1976, *J. nucl. Mater.*, **63,** 1.

CONN, R. W., KULCINSKI, G. L., and MAYNARD, C. W., 1978, *NUWMAK: An Attractive Medium Field, Medium Size, Conceptual Tokamak Reactor*, Univ. of Wisconsin Report, UWFDM-249.

CORBETT, J. W., and IANNIELLO, L. C., eds., 1972, *Radiation Induced Voids in Metals*, USAEC-Symp. Series 26.

DORAN, D. G., *et al.*, 1973, *Report of the Working Group on Displacement Models and Procedures for Damage Calculations*, Hanford Engineering Laboratory Report, HEDL-TME 73–76.

EMMETT, J. L., 1978, Progress in laser fusion research, given at the *7th Int. Conf. on Plasma Physics and Controlled Nuclear Fusion Research*, (Innsbruck, Austria (Vienna: IAEA)(to be published).

EUBANK, H., *et al.*, 1978, PLT neutral beam heating results, paper IAEA-CN-37-C-3 presented at the *1978 Plasma Physics and Controlled Thermonuclear Research in Innsbruck, Austria* (Vienna: IAEA) (to be published).

EVANS, R. D., 1955, *The Atomic Nucleus*, (New York: McGraw-Hill).

FISH, R. L., STRAALSUND, J. L., HUNTER, C. W., and HOLMES, J. J., 1973, *Effects of Radiation on Substructure and Mechanical Properties of Metals and Alloys*, ASTM-STP-529, Am. Soc. for Testing and Materials.

FRAAS, A. P., 1973, *Conceptual Design Study of the Blanket and Shield Region and Related Systems for a Full Scale Toroidal Fusion Reactor*, Oak Ridge National Lab., Report ORNL-TM-3096.

FRANK, T., *et al.*, 1974, *Proc. 1st Topical Mtg. on Tech. of Controlled Nucl. Fusion*, ed. G. R. Hopkins, Conf-740702, p. 83.

GABRIEL, T. A., BISHOP, B. L., and WIFFEN, F. W., 1978, *Alloy Development for Irradiation Performance*, Dept. of Energy Report, DOE/ET-0058/1, p. 30.

GHONIEM, N. M., and KULCINSKI, G. L., 1978, *J. nucl. Mater.*, **69/70,** 816.

GHONIEM, N. M., and KULCINSKI, G. L., *J. nucl. Mater.* (to be published).

GILBERT, E. R., KAULITZ, D. C., HOLMES, J. J., CLAUDSON, T. T., 1972, *Irradiation Embrittlement and Creep in Fuel Cladding and Core Components* (London: British Nuclear Energy Society), p. 239.

HOVINGH, H., 1977, *Proc. of 2nd Topical Mtg. on Tech. of Controlled Nucl Fusion*, ed. G. L. KULCINSKI, CONF-760935-P2, p. 765.

HUNTER, T. O., and KULCINSKI, G. L., 1978 a, *Description of the Response of Materials to Pulsed Thermonuclear Radiation* (Part III), University of Wisconsin Report, UWFDM-232.

HUNTER, T. O., and KULCINSKI, G. L., 1978 b, *The T-DAMEN Computer Code*, University of Wisconsin Report, UWFDM-247.

HUNTER, T. O., and KULCINSKI, G. L., 1978 c, *J. nuel. Mater.*, **76/77,** 383.

HUNTER, T. O., and KULCINSKI, G. L., 1978 d, *Fusion Reactor Design Concepts*, Int. At. Energy Agency, Vienna, p. 561.

KAMINSKY, M., ed., 1965, *Atomic and Ionic Impact Phenomena on Metal Surfaces* (Berlin: Springer-Verlag).

KAMINSKY, M., ed., 1976, *Radiation Effects on Solid Surfaces*, (Washington, D.C.: American Chemical Society) Advances in Chemistry Series-158.

KRAMER, D., *et al.*, 1968, *J. nucl. Mater.*, **25,** 121.

KULCINSKI, G. L., 1974, Radiation effects and tritium technology for fusion reactors, *Proc. Int. Conf., Gatlinburg, Tenn.*, ed. J. S. Watson and F. W. Wiffen, CONF-750989, p. I-17.

KULCINSKI, G. L., 1975, *Plasma Physics and Controlled Thermonuclear Research* 1974, Vol. II (Vienna: IAEA), p. 251.

KULCINSKI, G. L., 1978a, in *Fusion Reactor Design Concepts*, (Vienna: IAEA), p. 573.

KULCINSKI, G. L., 1978b, *Tokamak Reactors for Breakeven*, ed. H. Knoepfel (Oxford: Pergamon Press), p. 449.

KULCINSKI, G. L., 1978. P. 598 in *Proc. 3rd Topical Meeting on Technology of Controlled Nuclear Fusion*, ed. J. R. Powell, CONF-780508.

KULCINSKI, G. L., ABDOU, M., and DORAN, D. G., 1975, *Properties of Reactor Structural Alloys After Neutron or Particle Irradiation*, ASTM Special Technical Publication-570 (Philadelphia: ASTM), p. 239.

MANISCALCO, J. A., MEIER, W. R., and MONSLER, M. J., 1977, *Trans. Am. Nucl. Soc.*, **27,** 34.

MATTAS, R. F., and SMITH, D. L., 1978, *Nucl. Tech.*, **39,** 186.

MATTHEWS, J. R., 1977, *Contemp. Phys.*, **18,** 571.

MAZIASZ, P. J., WIFFEN, F. W., and BLOOM, E. E., 1976, *Radiation Effects and Iritium Technology for Fusion Reactors*, ed. J. S. Watson and F. W. Wiffen, CONF-750989 (Springfield, VA: NTIS), p. I-259.

MCCARVILLE, T., HASSANIEN, A. M., and KULCINSKI, G. L. 1978. Univ. of Wisconsin Report, UWFDM-282.

MILLS, R. G., ed., 1974, *A Fusion Power Plant*, Princeton Plasma Physics Report, MATT-1050.

MOIR, R. W., 1976, *J. nucl. Mater.*, **63,** 21.

NELSON, R. S., 1965, *Phil. Mag.*, **11,** 291.

NELSON, R. S., ed., 1975, *Physics of Irradiation Produced Voids*, Harwell Report, AERE-R-7934.

NUCKOLLS, J., *et al.*, 1978. Laser Program Annual Report—1977, p. 4–19 in Vol. 2, UCRL-50021–77, Lawrence Livermore Laboratory Report.

ODETTE, G. R., and DOIRON, D. R., 1976, *Nuclear Technology*, **29,** 346.

RIBE, F. L., 1974, *Fusion Reactor Design Problems* (*Nuclear Fusion* Special Supplement), p. 99.

SIMONEN, T. C., *et al.*, 1978, UCRL-80634, Lawrence Livermore Laboratory Report.

STEINER, D., 1977, *ORNL Fusion Power Demonstration Study: Interim Report*, Oak Ridge Report, ORNL-TM-5813.

SZE, D., unpublished work, 1978.

THOMPSON, S. L., 1973, *Improvements in the CHART-D Energy Flow Hydrodynamic Code V*, Sandia Laboratory Report, SLA-73-0477.

VOGELSANG, W. F., KULCINSKI, G. L., LOTT, R. G., and SUNG, T. Y., 1974, *Nucl. Tech.*, **22,** 279.

WERNER, R. W., *et al.*, 1974, *Fusion Reactor Design Problems* (*Nuclear Fusion* Special Supplement), p. 171.

WIEDERSICH, H., KAMINSKY, M. S., and ZWILSKY, K. M., eds., 1974, Surface Effects in Controlled Fusion, *J. nucl. Mater.*, **53.**

WIFFEN, F. W., and BLOOM, E. E., 1974, ORNL-TM-4541.

WIFFEN, F. W., and STIEGLER, J. O., 1977, *Proc. of 2nd Topical Meeting on the Technology of Controlled Nuclear Fusion*, ed. G. L. Kulcinski, CONF-760935-P2, p. 135.

1974, *Fusion Reactor Design Problems*, Special Supplement to *Nuclear Fusion*, (Vienna: IAEA).

1978, *Fusion Reactor Design Concepts*, (Vienna: IAEA).